Multiscale Modeling of Carbon Nanotube Bundle Agglomeration inside a Gas Phase Pyrolysis Reactor

Guangfeng Hou[1*], Vianessa Ng[1], Chenhao Xu[1], Lu Zhang[2], Guangqi Zhang[1], Vesselin Shanov[1], David Mast[3], Wookyun Kim[1], Mark Schulz[1†], Yijun Liu[1]

[1] Department of Mechanical and Materials Engineering, University of Cincinnati, OH 45221, United States
[2] Department of Chemical and Biomolecular Engineering, University of California, Los Angeles, CA 90095, United States
[3] Department of Physics, University of Cincinnati, OH 45221, United States

ABSTRACT

Carbon nanotube (CNT) sock formation is required for the continuous synthesis of CNT thread or sheet using the gas phase pyrolysis method. Nanometer diameter CNTs form and are carried along the reactor tube by gas flow. During the flow, the CNT stick to each other and form bundles of about 10-100 nm diameter. Coupling of the CNT bundles in the flow leads to the formation of a centimeter diameter CNT sock with a wall that is hundreds of nanometers thick. Understanding the multiscale phenomena of sock formation is vital for optimizing the CNT synthesis and manufacturing process. In this work, we present a multiscale model for the CNT bundle agglomeration inside a horizontal gas phase pyrolysis reactor. The interaction between CNT bundles was analyzed by representing the attraction forces between CNTs using a discrete phase modeling method. Flow in the synthesis reactor was studied using a computational fluid dynamics (CFD) technique with multiphase flow analysis. A model was proposed to represent the coupling between CNT bundles and the gas flow. The effect of different CNT bundles on the agglomeration phenomenon was analyzed. The modeling results were also compared with experimental observations.

INTRODUCTION

Carbon nanotubes (CNTs) are being widely used in various engineering application areas such as electronics [1], composites [2-3], biosensors [4], and in the energy fields [5]. There are also large efforts toward the commercialization of CNT materials [6-7]. Among the CNT synthesis methods, the gas phase pyrolysis technique (also called floating catalyst method) holds high promise for large-scale production due to its ability for continuous synthesis. During the gas phase pyrolysis synthesis process, an aerogel-like sock [8-9] forms inside the reactor, which is critical for successful collection of CNT sheet and yarn. The CNT sock has a multiscale hierarchical structure, and it is formed from a large number of CNT bundles. These bundles are composed of individual CNTs held together due to van der Waals attractions. There are several studies discussing the agglomeration mechanism of these CNT bundles [10-13]. However, there are no attempts to model this agglomeration process directly. Detailed modeling and analysis of

---

* Corresponding author. Email: hougg@mail.uc.edu.
† Corresponding author. Email: Mark.J.Schulz@uc.edu.

CNT agglomeration and sock formation is highly desired in order to understand the synthesis process and to scale up the manufacturing process.

In this paper, a multiscale model is proposed to investigate the CNT bundle agglomeration process inside a horizontal gas phase pyrolysis reactor. The CNT bundles are modeled as spheres. The inter-bundle interaction and fluid-bundle interaction were studied through simulations. The simulation results are compared with experimental observations.

EXPERIMENT AND SIMULATION

In this study, a horizontal gas phase pyrolysis reactor is employed. The feedstock is injected into a 1400 °C reactor along with argon as a carrier gas, followed by the CNT growth and sock formation. The detailed conditions were reported in our previous work [10]. A commercial package COMSOL was used for the simulation studies.

RESULTS AND DISCUSSION

Multiscale structure of the CNT sock

The characteristics of CNT bundles are described along with their modeling. The CNT aerogel-like sock formed inside the reactor has multiscale hierarchical structure (Figure 1). The nanoscale CNT bundles are carried down the reactor by the fluid flow. The bundles then interact with each other and form microscale networks. These networks further entangle to form the CNT sock.
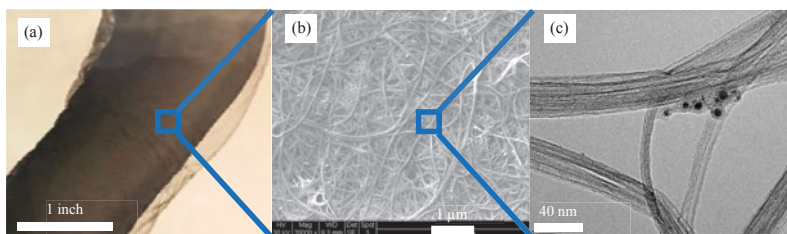

Figure 1. CNT sock and bundles: (a) CNT sock outside the reactor; (b) μm scale network; (c) TEM image of CNT bundles.

In the CNT sock, CNTs exist in the form of bundles. Bundle size depends on the number of CNTs in the bundle, and the diameter is around 50 nm. Van der Waals (vdW) and Casimir attraction could bridge different CNTs together and form bundles. Both vdW and Casimir forces are due to the electromagnetic mode fluctuations captured via the dielectric and magnetic response properties of the CNTs [14]. If the distance between CNTs is small (Angstrom to a few nm scale) where the retardation effects due to the finite speed of light can be neglected, the vdW force is characteristic. The Casimir regime is for large enough distance (sub-μm and μm scales) where retardation effects become important [15].

The CNT volume fraction inside the reactor can be estimated from the sock dimension and dynamics. For a typical sock, its diameter D is equal to the inner diameter of the ceramic tube. Its moving velocity u can be calculated by the carrier gas flowrate. This sock is continuously

collected on a drum with process yield of Y ($m_{CNT}/\Delta t$). To calculate the CNT volume fraction, we will consider the mass of the sock m_{CNT} produced during time period Δt (Figure 2).
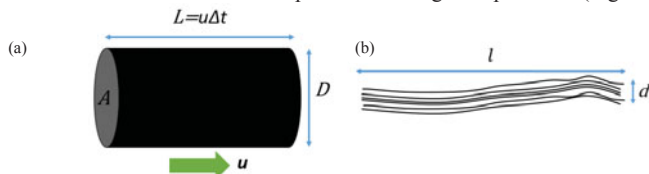

Figure 2. Illustration of the moving sock inside the reactor tube: (a) geometry and velocity of sock; (b) geometry of the CNT bundle.

The volume of the sock at time period Δt equals to $V_{sock} = u \cdot \Delta t \cdot \pi D^2 / 4$, and the volume of the CNTs can be estimated to be $V_{CNT} = m_{CNT} / \rho_{CNT} = Y \cdot \Delta t / \rho_{CNT}$. From these two equations, the CNT volume fraction can be calculated as: $\phi_{CNT} = \dfrac{V_{CNT}}{V_{sock}} = \dfrac{4Y}{\pi D^2 \cdot u \cdot \rho_{CNT}}$.

Table 1. Values used for calculating CNT volume fraction.

Parameter	Value
Y-process yield	1.06×10^{-7} kg/s
D-reactor ID	0.04445 m
u –carrier gas velocity	0.16 m/s [9]
ρ_{CNT}	1.8×10^6 g/m^3 [16]

Using the relevant values (Table 1), the CNT volume fraction Φ_{CNT} is around 2.36×10^{-7} inside the reactor tube. By assuming a CNT bundle diameter d of 50 nm and length l of 500 μm, the CNT bundle number density n_V is around 2.4×10^{11} per m^3. The number of CNT bundles in the sock cross-section can be estimated as; $\dfrac{D^2}{d^2} \cdot \Phi_{CNT} = 1.87 \times 10^5$, under the assumption that the CNT surface area fraction is the same as the volume fraction. The flow system is semi-dilute since $n_V l^3 = 30$, which is between 1 and l/d (10000) [17-18]. The number of particles passing through the reactor cross-section at unit time n_t can be estimated. Consider a time period Δt, during which the total number of particles passing through the reactor equals $n_t \Delta t$. During this period, the particles travel a distance of $u\Delta t$ which forms a volume of $u\Delta tA$, where A is the cross-section area of the reactor tube. With the number density definition, $n_t \cdot \Delta t = u \cdot \Delta t \cdot A \cdot n_V$; then

$$n_t = u \cdot A \cdot n_V = 5.97\times10^7 \text{ \#/s}.$$
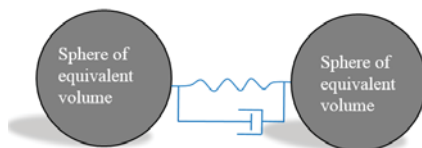
CNT bundle modeling

Figure 3. CNT bundle model.

In this study, the CNT bundles are simplified as spherical particles with the same volume as the bundle, where the spheres have an equivalent diameter d_p =1.23 μm (Figure 3). The CNT bundle motion inside the reactor is modeled using Newton's second law, and considering the drag force, thermophoretic force and inter-particle force [19] as:

$$\frac{d}{dt}(m_p \mathbf{v}) = \frac{3\mu C_D \text{Re}_r}{4\rho_p d_p^2} m_p (\mathbf{u}-\mathbf{v}) + \frac{6\pi k / k_p \cdot d_p \mu^2 C_s \nabla T}{\rho(2k / k_p +1)T} + \mathbf{F}_{inter} \qquad (1)$$

where the first term on the right side of the equation is the drag force and the second term is thermophoretic force, and m_p is the particle mass, d_p is the diameter of the volume equivalent sphere, μ is dynamic viscosity, $\mathbf{u}$ is fluid velocity, $\mathbf{v}$ is particle velocity, k is the thermal conductivity of the fluid, k_p is the particle thermal conductivity, T is the fluid temperature, ρ is fluid density, ρ_p is the particle density, and C_s is thermophoretic correction factor. The third term is the inter-particle force. The drag force was calculated using the Haider-Levenspiel model for non-spherical particles. In this equation, the Reynolds number is calculated as $\text{Re}_r = \rho \|\mathbf{u}-\mathbf{v}\| d_p / \mu$, and C_D is the drag coefficient, which depends on the sphericity factor (the ratio of the surface area of a volume equivalent sphere to the surface area of the considered non-spherical particle $S_p = A_{sphere} / A_{bundle}$).

The CNT inter-bundle interaction is modeled using a spring-dashpot method with a spring force and a damping dissipation force, which were originally developed for soft particle interactions [20]. Here a modified model is used for CNT bundles interaction:

$$\mathbf{F}_{inter}^i = -\sum_{j\neq i}^{N} k(\Delta r - r_0) - \eta(\mathbf{u}_i - \mathbf{u}_j) \qquad (2)$$

where k is the spring constant, Δr is the distance between two particles, r_0 is the equilibrium distance, and η is the damping coefficient. The purpose of this inter-particle force is to keep two particles together when they almost make contact. For efficient calculation, the equilibrium distance is set to 10 nm and the inter-particle interaction is only calculated within a cut-off distance of 100 nm. At higher gas flow, the CNT sock breaks due to high drag force, which can be estimated to be ~2.37×10⁻⁹ N for one particle (4000 sccm Ar flow). Considering two particles, the drag force on one particle has to be higher than the spring force and dissipation force at extreme cases to separate these two particles. This extreme case is used to estimate the spring constant and dissipation coefficient. The estimated value of k is 0.021 N/m and η is 4.9×10⁻¹⁰ N.s/m, which are used in the subsequent simulation.

The coupling of the CNT bundles and the gas flow can be modeled with the volume force generated by the particle motion [19] $F_v(\mathbf{r}) = -\sum_i F_d \delta(\mathbf{r} - \mathbf{q}_i)$. Here $\mathbf{q}_i$ is the particle position, and F_d is the drag force contribution of the particle motion to the volume force acting on the fluid.

CNT bundle agglomeration

The commercial software COMSOL was used for the simulation with the above equations. For the dilute case ($n_Vl^3=0.3$), the simulation result agrees qualitatively with the experimental observation (Figure 4). The calculated drag force on the individual particle is at a range of 3.9×10⁻¹⁰-9.7×10⁻⁶ μN and the thermophoretic force is 4.9×10⁻¹²-1.7×10⁻¹⁰ μN. In general, the drag force dominates, but the higher range of thermophoretic force is comparable to the lower range of drag force. Thus both forces contribute to the agglomeration process.
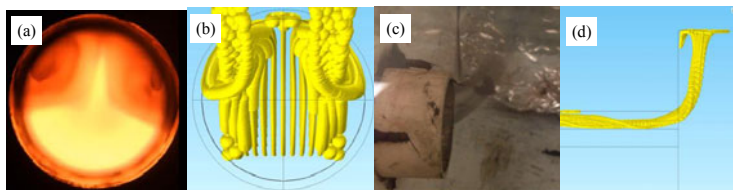
Figure 4. CNT bundle agglomeration for the dilute case: (a) experimental observation, side view; (b) simulation side view; (c) experimental observation, front view; (d) simulation front view.

For the semi-dilute case ($n_Vl^3=30$), the CNT sock morphology changes due to the strong interaction between CNT bundles. This has not been fully resolved by the simulation (Figure 5). Because of the bundle's high aspect ratio (10^2-10^5), one CNT bundle could interact with thousands of other bundles and form a macro network. This long-range interaction along the bundle axis has been simplified as an interaction between spheres. This simplification leads to the discrepancy between the experiment and simulation. An advanced model is under development to resolve this issue. One possible route is to use cylindrical rods with the correct aspect ratio of the bundles.
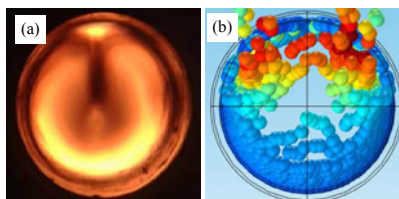

Figure 5. CNT bundle agglomeration for the semi-dilute case: (a) experimental; (b) simulation result.

CONCLUSIONS

In this work, the multiscale structure of the CNT sock was analyzed. The CNT bundle agglomeration process was simulated using a discrete particle method. The inter-particle interaction and fluid-particle interaction were modeled. There is good agreement between the experiment and simulation results for the dilute condition. The long-range interaction between bundles must be considered to more accurately represent the agglomeration process for the semi-dilute and dense flow conditions.

ACKNOWLEDGEMENTS

2625

REFERENCES

1. Chen, K. *et al.* Printed carbon nanotube electronics and sensor systems. *Adv. Mater.* **28,** 4397–4414 (2016).
2. Song, Y. *et al.* Carbon Nanotube Sheet Reinforced Laminated Composites. in *ASC 31st Technical Conference, Willamsburg VA* (2016).
3. Chauhan, D. *et al.* Multifunctional smart composites with integrated carbon nanotube yarn and sheet. in (eds. Leo, D. J. & Tarazaga, P. A.) **10172,** 1017205 (2017).
4. Hou, G., Zhang, L., Ng, V., Wu, Z. & Schulz, M. Review of Recent Advances in Carbon Nanotube Biosensors Based on Field-Effect Transistors. *Nano Life* **6,** 1642006 (2016).
5. Yehezkel, S., Auinat, M., Sezin, N., Starosvetsky, D. & Ein-Eli, Y. Bundled and densified carbon nanotubes (CNT) fabrics as flexible ultra-light weight Li-ion battery anode current collectors. *J. Power Sources* **312,** 109–115 (2016).
6. De Volder, M. F. L., Tawfick, S. H., Baughman, R. H. & Hart, a. J. Carbon Nanotubes: Present and Future Commercial Applications. *Science (80-.).* **339,** 535–539 (2013).
7. Schulz, M. J. *et al.* New Applications and Techniques for Nanotube Superfiber Development. *Nanotub. Superfiber Mater. Chang. Eng. Des*, 1st ed. (William Andrew Publishing, Boston, 2014) p. 33–59.
8. Koziol, K. *et al.* High-performance carbon nanotube fiber. *Science* **318,** 1892–5 (2007).
9. Hou, G. *et al.* Numerical and Experimental Investigation of Carbon Nanotube Sock Formation. *MRS Advances*, 2(1), 21-26 (2016).
10. Hou, G. *et al.* The effect of a convection vortex on sock formation in the floating catalyst method for carbon nanotube synthesis. *Carbon N. Y.* **102,** 513–519 (2016).
11. Conroy, D., Moisala, A., Cardoso, S., Windle, A. & Davidson, J. Carbon nanotube reactor: Ferrocene decomposition, iron particle growth, nanotube aggregation and scale-up. *Chem. Eng. Sci.* **65,** 2965–2977 (2010).
12. Chaffee, J. *et al.* Direct Synthesis of CNT Yarns and Sheets. *Nsti Nanotech 2008, Vol 3, Tech. Proc.* **3,** 118–121 (2008).
13. Zhong, X. H. *et al.* Continuous multilayered carbon nanotube yarns. *Adv. Mater.* **22,** 692–696 (2010).
14. Phan, A. D., Woods, L. M., Drosdoff, D., Bondarev, I. V. & Viet, N. A. Temperature dependent graphene suspension due to thermal Casimir interaction. *Appl. Phys. Lett.* **101,** 2–5 (2012).
15. Woods, L. M. *et al.* Materials perspective on Casimir and van der Waals interactions. *Rev. Mod. Phys.* **88,** 45003 (2016).
16. Laurent, C., Flahaut, E. & Peigney, A. The weight and density of carbon nanotubes versus the number of walls and diameter. *Carbon N. Y.* **48,** 2994–2996 (2010).
17. Yamane, Y., Kaneda, Y. & Dio, M. Numerical simulation of semi-dilute suspensions of rodlike particles in shear flow. *J. Nonnewton. Fluid Mech.* **54,** 405–421 (1994).
18. Krochak, P. J., Olson, J. a. & Martinez, D. M. Near-wall estimates of the concentration and orientation distribution of a semi-dilute rigid fibre suspension in Poiseuille flow. *J. Fluid Mech.* **653,** 431–462 (2010).
19. COMSOL. Particle Tracing Module Users Guide. (2015) p.153.
20. Tanaka, T., Kawaguchi, T. & Tsuji, Y. Discrete Particle Simulation of Flow Patterns in Two-Dimensional Gas Fluidized Beds. *Int. J. Mod. Phys. B* **7,** 1889–1898 (1993).